

Experimental and simulation studies of gas sorption processes in polycarbonate films

M. Mar López-González^{a,*}, Enrique Saiz^b, Evaristo Riande^a

^a*Instituto de Ciencia y Tecnología de Polímeros (CSIC), Juan de la Cierva 3, 28006 Madrid, Spain*

^b*Departamento de Química Física, Universidad de Alcalá, Alcalá de Henares, Madrid, Spain*

Available online 13 April 2005

It is a pleasure for us to dedicate this paper to Prof. James E. Mark on his 70th birthday.

Abstract

This work reports the experimental isotherms describing the concentration of oxygen and nitrogen in poly(bisphenol A carbonate-co-4,4'-(3,3,5-trimethylcyclohexylidene) diphenol carbonate) vs pressure, at 30 °C. The solubility coefficients are interpreted in terms of the Flory–Huggins theory, obtaining reasonable values for the enthalpic polymer–gas parameter. A new method is outlined to simulate the probabilities of inserting/removing a gas molecule in a host matrix already containing n molecules of gas. The simulated isotherms representing the pressure dependence of the concentration exhibit the same pattern as those experimentally obtained.

© 2005 Elsevier Ltd. All rights reserved.

Keywords: Experimental isotherms; Flory–Huggins theory; Polycarbonate

1. Introduction

As a result of the ever-growing industrial application of membranes technology in separation processes, the study of gas transport in membranes is a subject of great interest [1]. The permselectivity coefficient expressing membrane performance for gases separation is usually expressed in terms of the ratios of the permeability coefficients, that is:

$$\alpha_{(A/B)} = \frac{P_A}{P_B} = \frac{S_A}{S_B} \frac{D_A}{D_B} \quad (1)$$

where A and B are gases to be separated and P , S and D represent, respectively, the permeability, solubility and diffusion coefficients. The S_A/S_B ratio is one of the factors; other is the diffusion, which conditions the permselectivity performance of membranes. Both sorption and diffusion depend on the state of the membrane: rubbery amorphous, semi-crystalline and glassy. Since crystalline entities are opaque to gas transport and the discriminatory character of the diffusive process is rather small in rubbery membranes,

gas separation processes are mostly carried out through membranes in the glassy state [1].

Gas solubility in monomer liquids follows Henry's law while the solubility in rubbery polymers may in principle be obtained from the free energy of mixture between the gas in liquid form and the polymer chains [2,3]. However, there is no theory allowing the prediction of the solubility of gases in glassy membranes. An inspection of the shape of the isotherms representing the pressure dependence of the concentration of gas in polymers show a sharp increase in concentration at low pressures followed by a nearly linear increase of concentration with pressure at high pressures. This behaviour is usually interpreted in terms of the dual-mode model that assumes the glassy state as formed by a continuous phase in which microvoids accounting for the excess volume are dispersed [4]. Gas solubility obeys Henry behaviour in the continuous phase whilst the microvoids act as Langmuir sites where the molecules of gas are retained. According to the model, the solubility coefficient is given by [4,5]

$$S = k_D + \frac{bC'_H}{1 + bp} \quad (2)$$

where k_D is Henry's constant, C'_H is the concentration of gas in Langmuir sites and b is the polymer–gas parameter.

Simulation methods for gas transport through polymer

* Corresponding author.

membranes based on the Transition States Approach have been reported. According to the theory, the solubility coefficient is given by [6]

$$S = \frac{1}{kTV} \int_V \exp(-\Delta F/kT) dV \quad (3)$$

where kT is the thermal energy, V is the volume of the matrix and ΔF is the change in free energy taking place in the system by effect of the incorporation of molecules of gas in the free volume of the polymer matrix. A shortcoming of this method is that the solubility coefficient thus obtained is independent on pressure, in opposition with what occurs in glassy systems. Therefore we explore in this paper alternative methods to simulate gas solubility in glassy polymers. For this purpose we have measured the solubility of oxygen and nitrogen in poly(bisphenol A carbonate-co-4,4'-(3,3,5-trimethylcyclohexylidene)diphenol carbonate) (PBCDC). A schematic representation of the repeating unit of this polymer is shown in Fig. 1. The results were interpreted in terms of the dual mode model and further simulated using procedures based on the Widom method [7].

2. Experimental part

Pellets of PBCDC, supplied by Aldrich, were used to prepare films by compression molding. The time of residence of the film in the mold was 15 min and then the film was quenched in cold water. The glass transition temperature of PBCDC was measured with DSC 7 Perkin–Elmer calorimeter at a heating rate of 10 °C/min. The glass transition temperature, taken as the temperature at thermogram in the glassy region departs from the baseline, was 205 °C.

Gas sorption results were obtained in an experimental device, immersed in a thermostat, made up of a reservoir separated from the sorption chamber by a valve. The reservoir and sorption chamber were equipped, respectively, with Gometrics (0–35 bars) and Ruska model 7230 (0–35 × 10³ Torr) pressure sensors. Vacuum was made in both the reservoir and the sorption chamber containing the polymer

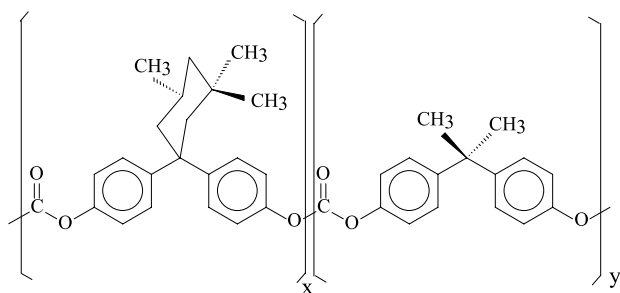


Fig. 1. Repeating unit of poly(bisphenol A carbonate-co-4,4'-(3,3,5-trimethyl cyclohexylidene) diphenol carbonate), PBCDC.

at 60 °C for about 6 h. Then the valve separating both chambers was closed and the pertinent gas was introduced into the reservoir. Once the reservoir reached the temperature of interest, the gas was allowed to flow to the sorption chamber by opening and closing nearly instantaneously the valve separate them. The sorption process was recorded every second with a PC via a MKS power supply/readout unit.

3. Experimental results and discussion

Values at 30 °C of the concentration of oxygen and nitrogen in PBCDC films are shown as a function of pressure in Fig. 2. As usual in glassy polymers, the isotherms are concave with respect to the abscissa axis. Eq. (2) fits the sorption results for oxygen and nitrogen using the Henry and Langmuir parameters given in Table 1. The amount of gas molecules immobilised in the Langmuir sites is rather high taking into account the low condensabilities of oxygen and nitrogen. This behaviour is a consequence of the microvoids, which account for the excess volume and act as Langmuir sites. Then the gas concentration in these sites can in first approximation be written as [5,8]

$$C'_H = 22414 \frac{(\partial v/\partial T)_{T_g} - (\partial v/\partial T)_T}{\bar{V}_g} (T_g - T) \\ = \frac{22414(\alpha_{T_g} - \alpha_T)}{\bar{V}_g} (T_g - T) \quad (4)$$

In this expression T_g is the glass transition temperature, and $T < T_g$ is the working temperature. The parameters v and α are, respectively, the specific volume and expansion coefficient of the polymer and \bar{V}_g is the partial molar volume of the gas in liquid state. A plot of $C'_H \bar{V}_g / [22414 (\alpha_{T_g} - \alpha_T)]$ vs $(T_g - T)$ for the same gas in different polymers should be a straight line roughly intercepting the origin of

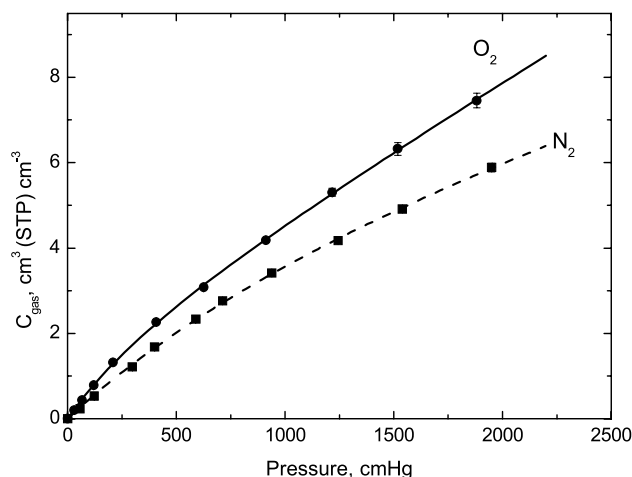


Fig. 2. Isotherms at 30 °C showing the variation with pressure of the concentration of oxygen and nitrogen in PBCDC films.

Table 1
Parameters for the dual model (Eq. (2)) calculated at 30 °C

	O ₂			N ₂		
	10 ³ k _D	C' _H	10 ³ b	10 ³ k _D	C' _H	10 ³ b
χ=0.0	1.54	2.68	6.90	0.944	1.97	6.39
χ=0.5	1.21	2.17	5.99	0.781	1.56	5.71
χ=1.0	0.959	1.66	6.29	0.683	1.09	6.33
Ideal gas	2.09	4.01	7.24	1.75	3.41	7.30
Fitting Eq. (2) to experimental results	3.02	2.18	2.03	1.30	6.64	0.53

the coordinates axes. Hence the higher T_g is the larger C'_H for a given gas should be.

The dual mode model assumption of a continuous phase obeying Henry behaviour led us to postulate the sorption processes in this region as governed by the free energy of mixture of the polymer with the gas in the liquid state. The use of the Flory–Huggins theory [9] to obtain the free energy of mixture leads to the following expression for the Henry's constant [3,10–12]

$$k_D = \frac{22414}{76V_p} \exp \left[-(1 + \chi) - \frac{\lambda}{RT_b} \left(1 - \frac{T_b}{T} \right) \right] \quad (5)$$

where \bar{V}_p is the partial molar volume of the gas in the liquid state in cm³/mol, T_b its boiling temperature at 1 atm in Kelvin, λ is the latent heat of vaporisation at T_b in cal/mol and χ is the dimensionless enthalpic gas (liquid)–polymer interaction parameter. The values of k_D obtained by fitting Eq. (2) to the sorption results, substituted into Eq. (5), give the values of χ . The values of this parameter for oxygen and nitrogen at 30 °C are 0.8 and 1.3, respectively. These values are in consonance with those obtained for polymer–liquid solutions using the Flory–Huggins theory.

3.1. Sorption and desorption simulations

The simulation of the sorption and desorption processes is performed in three consecutive steps. In the first place, the polymeric host matrix is prepared and the interactions among the atoms of the polymer matrix and one molecule of the guest gas to be absorbed are computed. Then, the probabilities of inserting and removing one molecule of the gas at different positions within the matrix are computed taking into account both energetic and geometric considerations. Finally, Monte Carlo sampling procedures are employed to perform attempts to both insert and remove one molecule of the gas at randomly chosen positions of the matrix until the final equilibrium is reached.

3.1.1. Preparation of the host polymer matrix and interaction with the guest gas molecules

The protocol used to prepare a cubic box containing the polymer with the desired density is fully described elsewhere [13–15]. Four H-terminated oligomers were

packed into a cubic box having periodic boundary conditions and box side length $L=33$ Å. A combination of simplex minimisation, annealing processes (simulated by molecular dynamics procedures) and conjugated gradients minimisation were employed for preparing an optimised structure of the matrix. The Amber force field [16–20] was employed to compute interatomic interactions. Partial charges were assigned to each atom of the matrix by means of the AMPAC-AM1 [21] procedure and employed to evaluate the Coulombic contributions to the potential energy [22].

A grid containing 10⁶ positions is then obtained by dividing each side of the cubic box in $G=100$ intervals of the same length and the centre of masses of the gas molecules is successively placed at each one of the grid positions and its interaction with the polymer matrix is computed.

The TSA theory assumes that the atoms of polymer oscillate over their equilibrium positions with a root mean-square value $\Delta \approx 0.3$ Å, so that the probability of finding atom i of the polymer matrix at a distance δ from its main position is given by [6–23]

$$W(\delta) \sim \exp \left(-\frac{\delta^2}{2\Delta^2} \right) \quad (6)$$

Consequently, if we assume that at a given moment one atom A of the gas molecule is located at a certain position with a equilibrium distance R_{Ai} from one atom i of the polymer, the actual distance r_{Ai} will fluctuate and so will the interaction among these two atoms E_{Ai} do. The distance r_{Ai} may be written as function of the equilibrium distance R_{Ai} , the radial displacement δ and the orientational angle θ' , as it is illustrated in Fig. 3. The interaction E_{Ai} could then be computed at a given value of R_{Ai} as function of δ and θ' and Boltzman factors of these energies, together with the probabilities dictated by Eq. (6) could be integrated over δ and θ , thus providing the partition function $Z_{Ai}(R_{Ai})$ and the free energy:

$$F_{Ai}(R_{Ai}) = -kT \ln[Z_{Ai}(R_{Ai})] \quad (7)$$

for the interaction among atom A of the gas molecule and atom i of the polymer. As Eq. (7) indicates, this free energy

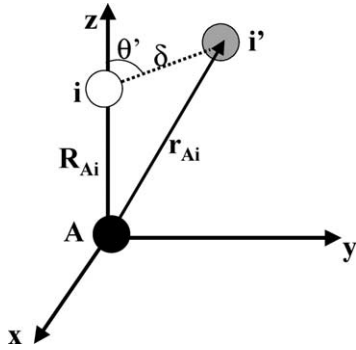


Fig. 3. Actual distance r_{Ai} between atom A of the gas molecule and polymeric atom i . It depends on the equilibrium distance between these two atoms R_{Ai} , the displacement of atom i from its equilibrium position δ and the orientational angle θ' .

depends only on the equilibrium distance between those two atoms.

It is further assumed that rotation of diatomic molecules is much faster than their translation, thus allowing energy averaging over all the permitted rotations for each position of the molecule. Let us focus on a molecule of a diatomic AB gas whose centre of masses is placed at a given grid position m . The orientation of this molecule with respect to all the atoms of the polymer matrix is governed by the ϕ and θ angles, as it is indicated in Fig. 4. Eq. (7) could then be used to compute the interactions among the atoms of the molecule and those of the polymer. Thus, the interaction between the molecule placed at grid position m with a given orientation ω , defined by a pair of values of ϕ and θ , and the whole polymer matrix is given by:

$$E_m(\omega) = \sum_i [F_{Ai}(R_{Ai}) + F_{Bi}(R_{Bi})] \quad (8)$$

where the sum expands over all the atoms of the polymer and the m subscript indicates the grid position where the centre of masses of the molecule is located.

The partition function for the molecule in grid position m

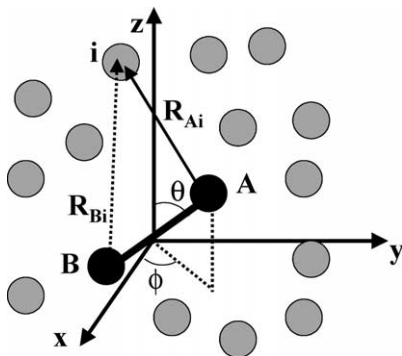


Fig. 4. A diatomic AB gas molecule with its centre of mass placed at one grid point within the polymeric matrix whose atoms are represented by gray circles. R_{Ai} and R_{Bi} represent the equilibrium distances between the atoms of the molecule and polymeric atom i . The orientation of the gas molecule is governed by the orientational angles ϕ and θ defined with respect to an arbitrary coordinates system affixed to its centre of masses.

may be obtained through integration over ϕ and θ , which define the orientation ω . Thus:

$$Z_m = \int_{\theta} \sin(\theta) d\theta \int_{\phi} \exp[-E_m(\omega)/kT] d\phi \quad (9)$$

Finally, the increment on the free energy of the system associated with insertion of one molecule of gas at grid position m is given by:

$$\Delta F_m = -kT \ln[Z_m] \quad (10)$$

It is important to realise that, even if only one configuration of the polymer matrix with fixed main positions is considered, allowance of the oscillation represented by Eq. (6) paramount to the evaluation of many different configurations with fully fixed atomic positions.

3.1.2. Statistical weights

Let us consider a polymer inside a cubic box in which vacuum was made. Then a certain gas at pressure p is allowed in. Under those circumstances, sorption and desorption processes continuously occur. At the beginning, the sorption rate is larger than the desorption rate and therefore, the number of gas molecules absorbed by the polymer increases until equilibrium is reached. At that moment, both rates become equal and the number of absorbed molecules N , remains constant. Let us consider a moment in which that $n < N$ molecules of gas are already inside the box. If we try to insert a new molecule at grid position m , thus increasing the occupation number from n to $n + 1$, the statistical weight associated with this insertion is given by [7,11]:

$$\sigma'_{i,n \rightarrow n+1} = \exp\left[-\frac{\mu(n+1) - \mu(N)}{kT}\right] \quad (11)$$

The change in chemical potential arises from both the variation of potential of the ideal gas and the inter-atomic interactions occurring by the action of inserting a molecule of gas in the box. Since the chemical potential of the ideal gas is:

$$\mu = \mu_0 + kT \ln C \quad (12)$$

where C is the concentration. Eq. (11) can alternatively be written as:

$$\sigma'_{i,n \rightarrow n+1} = \frac{N}{n+1} \exp\left(-\frac{\Delta F_m}{kT}\right) \quad (13)$$

where ΔF_m , given by Eq. (10), is the change in free energy associated with the insertion of one gas molecule at grid position m .

In the same way, the statistical weight associated with the removal of a molecule of gas from the box is expressed by:

$$\sigma'_{r,n \rightarrow n-1} = \frac{n-1}{N} \exp\left(\frac{\Delta F_m}{kT}\right) \quad (14)$$

In earlier works [13–15] we have taken N as the number of ideal gas molecules that would fill up the empty box at the given values of p and T . Thus, Eqs. (13) and (14) were written as:

$$\sigma'_{i,n \rightarrow n+1} = \frac{pV}{(n+1)kT} \exp\left(-\frac{\Delta F_m}{kT}\right) \quad (15)$$

$$\sigma'_{r,n \rightarrow n-1} = \frac{(n-1)kT}{pV} \exp\left(\frac{\Delta F_m}{kT}\right) \quad (16)$$

A more realistic approach, however, would be to obtain N from Henry's constant, which in turn can be estimated from Eq. (5). Taking this approach, Eqs. (13) and (14) become:

$$\sigma'_{i,n \rightarrow n+1} = \frac{pk_D}{n+1} \exp\left(-\frac{\Delta F_m}{kT}\right) \quad (17)$$

$$\sigma'_{r,n \rightarrow n-1} = \frac{n-1}{pk_D} \exp\left(\frac{\Delta F_m}{kT}\right) \quad (18)$$

It should be stressed that the statistical weights associated with the insertion and removal of molecules using Eqs. (17) and (18) are values in defect at low pressures due to the fact that, when p is small, the second term on Eq. (2) is important and consequently $k_D < S$. However, at moderate and high pressures, the values of k_D and S become closer, and, in fact, $k_D \rightarrow S$ when $p \rightarrow \infty$.

3.1.3. Geometric factors

The volume of the cubic box dictated by CPU considerations on the Molecular Dynamics simulations employed during the preparation of the polymer matrix, i.e. $V \approx 33^3 \text{ \AA}^3 \approx 3.6 \times 10^{-20} \text{ cm}^3$, is too small as to allow a reasonable Monte Carlo sampling. For instance, the equilibrium number of particles of an ideal gas under STP conditions contained in such a volume would be $N \approx 0.9$. In order to avoid this inconvenience, we set up an ensemble of $(N_{\text{box}})^3$ boxes identical to that containing the polymer matrix, packed within a cube with side LN_{box} . Thus, the volume appearing on Eqs. (15)–(18) is given by $(LN_{\text{box}})^3$ while each grid position is repeated $(N_{\text{box}})^3$ times with PBC conditions within the ensemble.

On the other hand, the volume of one gas molecule is much larger than the volume of one grid position. Thus, when the centre of masses of one molecule is placed at a given grid position, it in fact occupies a number of grid positions given by:

$$g = V_{\text{molec}} \left(\frac{G}{L}\right)^3 \quad (19)$$

where V_{molec} represents the volume of the molecule and G^3 is the number of grid positions within the primary box, i.e. the number of grid position in the whole ensemble of boxes would be $(GN_{\text{box}})^3$. Since we sample each individual grid position, the whole volume would be completely filled up when we succeed in 1 out of every g grid positions.

Consequently, a new statistical weight taking care of this effect is defined as:

$$\sigma''_{i,n \rightarrow n+1} = \frac{1}{g} = \frac{L^3}{V_{\text{molec}} G^3} \quad (20)$$

$$\sigma''_{r,n \rightarrow n-1} = g = V_{\text{molec}} \left(\frac{G}{L}\right)^3 \quad (21)$$

Combining Eqs. (17) and (18) with (20) and (21), the total statistical weight for insertion and removal of a gas molecule at grid position m when the system already contains n molecules is given by:

$$\sigma_{i,n \rightarrow n+1} = \frac{pk_D L^6 (N_{\text{box}})^3}{(n+1) V_{\text{molec}} G^3} \exp\left(-\frac{\Delta F_m}{kT}\right) \quad (22)$$

$$\sigma_{r,n \rightarrow n-1} = \frac{(n-1) V_{\text{molec}} G^3}{pk_D L^6 (N_{\text{box}})^3} \exp\left(\frac{\Delta F_m}{kT}\right) \quad (23)$$

where the position of the grid point m determines the value of ΔF_m computed according to Eq. (10).

The pertinent probabilities can be obtained by normalisation of the statistical weights yielding:

$$p_i = \frac{\sigma_i}{\sigma_i + \sigma_r} \quad p_r = \frac{\sigma_r}{\sigma_i + \sigma_r} \quad (24)$$

3.1.4. Monte Carlo sampling

Monte Carlo techniques were used to insert or remove a molecule of gas from the cubic box. Each MC simulation consisted in 50 independently generated series of of 3×10^6 cycles. At each cycle, a grid position m in the grid matrix was randomly selected [24] and a random number x within the interval $[0,1]$ was generated and compared with p_i (Eq. (24)). When $x \leq p_i$ an attempt to insert a new particle into position m was performed, otherwise, i.e. when $x > p_i$ removal of one particle from position m was attempted. The insertion fails if the new molecule has its centre of mass within a distance smaller than a molecular diameter from the centre of mass of any of the n previously loaded molecules; otherwise the insertion is successful. Molecular overlapping of guest molecules is rather infrequent because the number of molecules loaded into the matrix is much smaller than what would be allowed by the ratio among the volumes of the matrix and the molecule. For this reason no interactions among molecules of solute were considered when computing the values of ΔF appearing in Eqs. (13)–(18). On the other hand a removal attempt was successful when the centre of mass of the molecule lies within a distance smaller than the molecular radius from the tested position. Failed attempts to insert or remove gas molecules leaves the system unchanged.

The number of molecules loaded in the polymer matrix obtained in one of the 50 series is plotted as a function of the number of Monte Carlo cycles (MC) in Fig. 5. Horizontal lines on this figure represent the average obtained for the 50

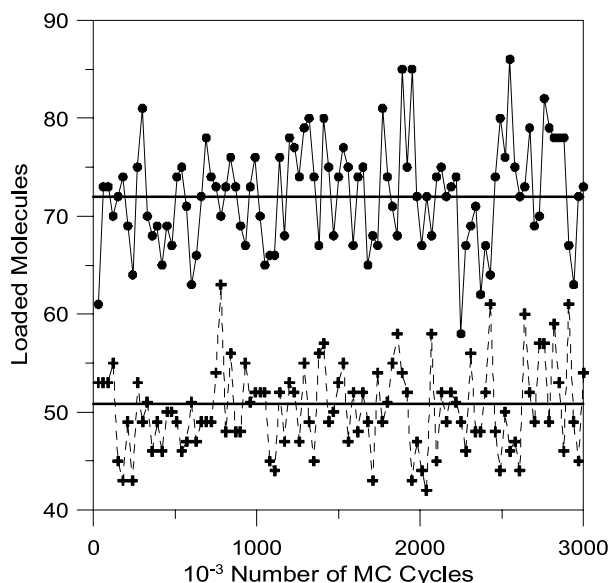


Fig. 5. Number of O₂ (circles) and N₂ (crosses) molecules loaded into the polymeric matrix as function of the Monte Carlo cycles for one of the 50 independent simulations performed to compute the solubility of the gases into the polymer. Horizontal lines represent the average obtained over the 50 simulations. Calculations were performed at 30 °C, $p=76$ cm Hg, $N_{\text{box}}=4$, $\chi=0$. See text for details.

series generated for each molecule. Computations were performed at 30 °C and 1 atm of pressure with $N_{\text{box}}=4$ and $\chi=0$. The results in Fig. 5 show that, although the number of loaded molecules computed in each individual run present random fluctuations, the averages over the 50 series performed for each system reach a roughly constant value after a few thousand of MC cycles. The variation of the concentration of oxygen and nitrogen in the polymer matrix is represented as a function of pressure in Figs. 6 and 7, respectively. Standard deviations on the averages amounted to ca. 5% and are represented by vertical bars. It is worth noting that the curves obtained exhibit the same pattern as the experimental gas sorption isotherms in the sense that they are concave with respect to the abscissa axis. Values of the computed dual mode parameters are shown in Table 1.

4. Discussion

As was indicated above, the simulation starts using Eq. (5) to estimate the number N of guest molecules at equilibrium. However, the value of this quantity depends on the enthalpic gas–polymer interaction whose value is in principle unknown. Since $k_D < S$, we felt we should take $\chi=0$ to estimate the value of Henry's constant. The effect of the enthalpic parameter on the simulated isotherms represented in Figs. 6 and 7 show that as χ increases, that is, the incompatibility between polymer-gas (liquid) increases, the concentration of gas decreases. Fairly good results are obtained for $\chi=0$. Taking a close look to the figures one can observe that the simulated values of the concentration

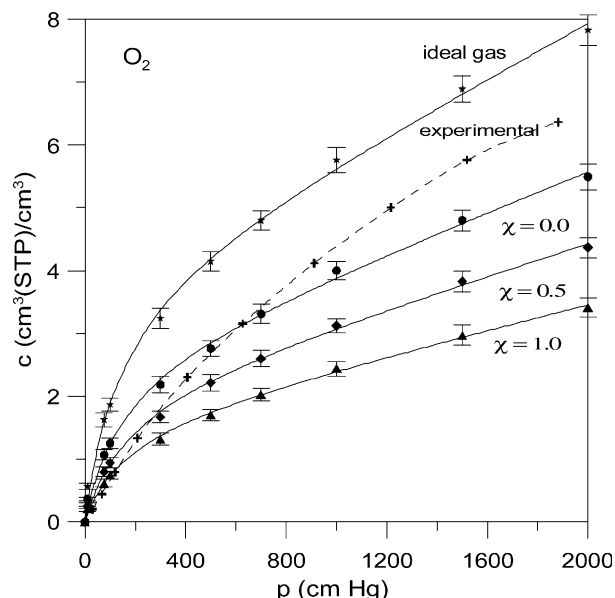


Fig. 6. Variation of the concentration of O₂ as function of pressure computed at 30 °C with several values of the Flory–Huggins parameter χ . Crosses indicate experimental results while the stars represent values obtained assuming that the box is filled up with molecules of ideal gas, i.e. employing Eqs. (15) and (16) instead of (17) and (18).

increases rather sharply with the pressure in comparison with the experimental results in the low pressure region [25]. The simulated concentration for large values of pressure comes closer to the experimental data in this region. However, departure from the experimental results at large pressures increases as χ increases. Overestimation of experimental solubilities by calculations performed at low pressures is quite frequent [15,25,26]. The reasons invoiced to explain this behaviour are inhomogeneities in the density of the simulated polymeric matrix and uncertainties arising

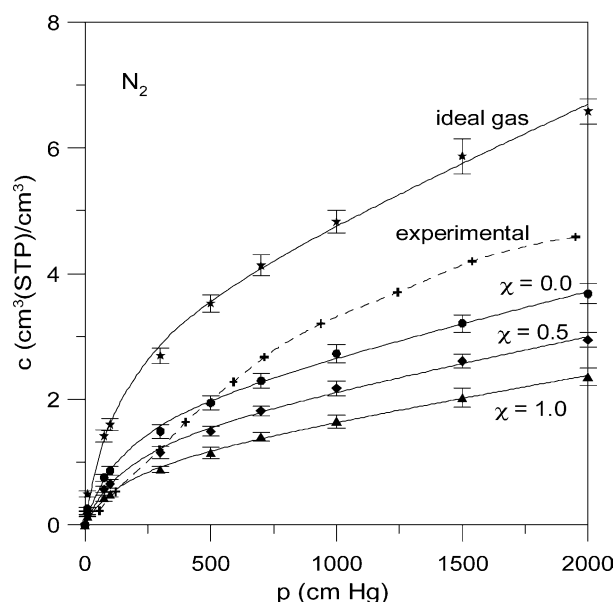


Fig. 7. Same as Fig. 6 for N₂.

from poor sampling when the equilibrium occupation is too small. Both effects become less important as the pressure increases.

Computations were also carried out using Eqs. (15) and (16) which extract the value of N assuming that the box is empty, an approach used earlier. The pertinent curves are shown in Figs. 6 and 7. It can be seen that the pressure dependence of the concentration at low pressures is too steeply in comparison with the experimental results. The simulation overestimates the concentration over all the range of pressures presumably as a consequence of the fact that the first factor in Eq. (15) (insertion) and (16) (removal) is, respectively, larger and smaller than the real one.

The simulated results for the solubility coefficient significantly differ from the experimental ones in the low-pressure region (see Figs. 8 and 9) where the adsorption contribution to the sorption process is important. This contribution becomes less and less important at pressures above 3 atm where Henry's contribution to the solubility is dominant. However, the difference between simulated and experimental values in the low pressures region considerably diminishes if N is estimated from Henry's constant, although some discrepancy still remains. The discrepancy observed may arise from polymer density being too inhomogeneous in samples prepared by simulations. Uncertainties arising from poor sampling due to small equilibrium occupation could also be the cause of the discrepancy.

5. Conclusions

The description of the change in free energy arising from the gas sorption process in the continuous phase of glassy membranes in terms of the Flory–Huggins theory of

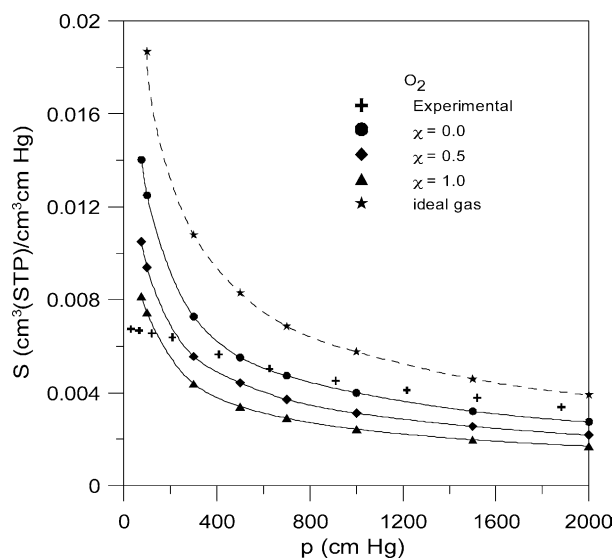


Fig. 8. Variation of the solubility of O_2 as function of pressure. See caption of Fig. 6.

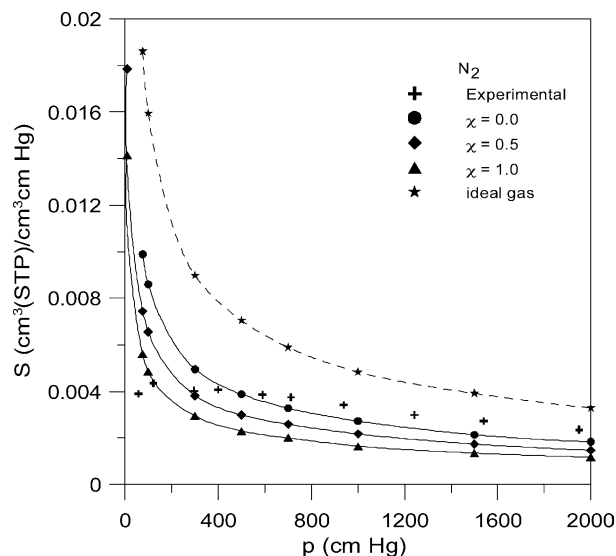


Fig. 9. Same as Fig. 8 for N_2 .

polymer gives reasonable values for the enthalpic polymer–gas (in liquid form) interaction. The value of Henry's constant estimated from this analysis is a good approach to estimate the gas ideal contribution to the statistical weights associated with both insertion and removal of gas molecules in the polymer matrix. The method described in this work to simulate gas sorption in polymers opens a promising way to simulate the solubility of gases as a function of the chemical structure of the host matrix and pressure.

Acknowledgements

Financial support provided by the DGICYT (Dirección General de Investigación Científica y Tecnológica) through Grants MAT2002-04042-CO2-02 and BQU2001-1158 is gratefully acknowledged.

References

- [1] Kesting RE, Fritzsche AK. Polymeric gas separation membranes. New York: Wiley-Interscience; 1993.
- [2] Petropoulos JH. Pure Appl Chem 1993;65:219.
- [3] López-González MM, Compañ V, Riande E. Macromolecules 2003; 36:8576.
- [4] Vieth WR, Sladek KJ. J Colloid Sci 1965;20:1014. Ref. 1; p. 60.
- [5] Koros WJ, Paul DR. J Polym Sci Part B Polym Phys 1978;16:1947.
- [6] Gusev AA, Müller-Plathe WF, van Gunsteren WF, Suter UW. Adv Polym Sci 1994;43:1977.
- [7] Widom BJ. Chem Phys 1963;39:2802.
- [8] Muruganandam N, Koros WJ, Paul DR. J Polym Sci Part B Polym Phys 1987;25:199.
- [9] Flory PJ. Principles of polymer chemistry. Ithaca, NY: Cornell University Press; 1953. Chapter 21.
- [10] Tlenkopatchev MA, Vargas J, López González M, Riande E. Macromolecules 2003;36:8483.
- [11] Tlenkopatchev MA, Vargas J, Alvarez-Girón MA, López-González M, Riande E. Macromolecules 2005 (in press).

- [12] The term T_b/T is erroneously inverted in Ref. [10].
- [13] López-González M, Saiz E, Guzmán J, Riande E. *Macromolecules* 2001;34:4999.
- [14] López-González M, Saiz E, Guzmán J, Riande E. *J Chem Phys* 2001; 115:6728.
- [15] Saiz E, López-González M, Riande E, Guzmán J, Compañ V. *Phys Chem Chem Phys* 2003;5:2862.
- [16] Weiner SJ, Kollman PA, Nguyen DT, Case DA, Singh UC, Ghio C, et al. *J Am Chem Soc* 1984;106:765.
- [17] Weiner SJ, Kollman PA, Nguyen DT, Case DA. *J Comp Chem* 1986; 7:230.
- [18] Homans SW. *Biochemistry* 1990;29:2110.
- [19] Cornell WD, Cieplak P, Bayly CL, Gould IR, Merz KM, Ferguson DMD, et al. *J Am Chem Soc* 1995;117:5179.
- [20] <http://www.amber.ucsf.edu/amber/amber.html>.
- [21] MOPAC, Department of Chemistry, Quantum Chemistry Program Exchangers, Indiana University, Bloomington, IN.
- [22] Forester TR, Smith W. DL_POLY, Version 2.10, Daresbury Laboratory, Warrington WA4 4AD, England.
- [23] Gusev AA, Suter UW. *J Comput-Aided Mater Des* 1993;1:63.
- [24] This method of insertion is not completely random, since only predetermined grid points, at which the interactions among guest molecules and host polymer matrix were computed in the previous step, are considered. A completely random insertion implies to compute those interactions at each new insertion and would require a prohibitively long computer time. At any rate, the separation between neighbor grid positions is ca. 0.33 Å, which is much smaller than the size of the inserted molecule, so that the insertion is very close to completely random.
- [25] Tiemblo P, Saiz E, Guzmán J, Riande E. *Macromolecules* 2002;35: 4167.
- [26] Muller-Plathe F. *Macromolecules* 1991;24:6475.